THE ASTRONOMICAL JOURNAL, 119:1638–1644, 2000 April

OPTICAL SURFACE PHOTOMETRY OF A SAMPLE OF DISK GALAXIES. I. OBSERVATIONS AND DATA REDUCTION[1]

J. A. L. AGUERRI, A. M. VARELA, M. PRIETO, AND C. MUÑOZ-TUÑÓN
Instituto de Astrofísica de Canarias, Calle Vía Láctea s/n, E-38200 La Laguna, Tenerife, Spain
Received 1998 June 30; accepted 2000 January 4

ABSTRACT

We present accurate optical surface photometry in the U, B, V, R, and I passbands for 11 disk galaxies. The sample has been selected in order to study the different morphological structures present in disk galaxies and includes all morphological types. For each galaxy, we present surface brightness, ellipticity, and position angle radial profiles from ellipse fits to the isophotes. Color index images and color index profiles in $U-B$, $B-V$, and $B-I$ are also shown. The photometric information obtained is crucial to understanding the different morphological structures presented in all these galaxies, and to obtain their mass distributions. The latter topic will be the subject of a forthcoming paper.

Key words: galaxies: photometry — galaxies: spiral — galaxies: structure

1. INTRODUCTION

Over the last few decades, bidimensional broadband photometry of disk galaxies has been used in order to arrive at a better understanding of galactic structure and dynamics. Such photometry has the advantage of being relatively easy to obtain and gives information about the spectral energy distribution of the object.

A great deal of information can be derived from broadband photometry, including the stellar population (Searle, Sargent, & Bagnuolo 1973; Peletier et al. 1994; Silva & Elston 1994), dust content (Evans 1994; Peletier et al. 1994, 1995; de Jong 1996b), and structure of galaxies by splitting the surface brightness profiles into their different components. These light profiles have often been decomposed only into a bulge and disk (Freeman 1970; Kormendy 1977; Boroson 1981; Kent 1986, 1987; Prieto et al. 1992; Caon, Capaccioli, & D'Onofrio 1993). Nevertheless, there are now available better fitting techniques and high spatial resolution photometry in the optical and near-infrared, which allow us to obtain more accurate photometric information on the structure of galaxies (Prieto et al. 1997; Wozniak et al. 1995; Elmegreen et al. 1996; de Jong 1996a). The photometric parameters describing the light distribution of the components are of fundamental importance in the study of galaxy formation and evolution. Moreover, the bulge-to-disk ratio is related to the Hubble classification scheme (Simien & de Vaucouleurs 1986; Andredakis & Sanders 1994; de Jong 1996a).

Knowledge of the geometries of different galactic components allows us to derive their spatial source distribution (Stark 1977; Varela 1992; Simonneau, Varela, & Muñoz-Tuñón 1993; Varela, Muñoz-Tuñón, & Simonneau 1996); by assuming a mass-to-light ratio for the galaxy (Rubin, Ford, & Thonnard 1980; Rubin et al. 1982, 1985), the gravitational potential can also be obtained (Freeman 1970; Hunter et al. 1988), which is essential to the understanding of galactic dynamics.

Our main goal is to perform a structural and dynamical study for a sample of spiral galaxies with different morphological types. We will make a detailed analysis of their structural components (e.g., disk, bulge, bar, ring, lens). The parameterization of these components will be made using ellipticity, position angle, and surface brightness isophotal profiles for those galaxies without bar structures. Radial surface brightness profiles along the bar axis will be used in the case of galaxies that have prominent bars. The deprojection of the observed photometric parameters will allow us to compute the three-dimensional structure of the bulge and bar, obtaining information about the spatial distribution. Applying different mass-to-light ratios to each component, we will obtain the mass distribution of each galaxy and their gravitational potentials. This will be the starting point to construct dynamical models for these galaxies.

In this first paper, we present the observations, the photometric information, and the two-dimensional characterization of all structural components that form the galaxies. In Paper II (Prieto et al. 2000), we will present the parameterization of these components. In a series of forthcoming papers we will develop the other issues.

2. OBSERVATIONS AND DATA REDUCTION

Eleven bright galaxies were observed in 1990 August. The sample was selected taking into account the following:

Morphological type.—The sample contains galaxies of all morphological types (from lenticular, e.g., NGC 6056, to late-type, e.g., NGC 6946), in order to observe all the different morphological structures present in spiral galaxies. The sample consists mainly of early-type galaxies with prominent bulges, since the main goal of the preliminary study was based upon a structural and morphological analysis of the bulge component, and on the search for triaxial structures and their dynamical consequences.

Inclination.—The galaxies selected have an intermediate inclination. This was chosen in order to obtain good velocity curves, either from the literature or from future observations.

Nuclear activity.—The galaxies have normal or low nuclear activity. No active galactic nuclei or starburst gal-

[1] Based on observations made with the Isaac Newton Telescope, operated on the island of La Palma by the Isaac Newton Group in the Spanish Observatorio del Roque de los Muchachos of the Instituto de Astrofísica de Canarias.

TABLE 1

GLOBAL PARAMETERS OF THE GALAXIES

Galaxy (1)	Type (2)	$\log D_{25}$ (3)	B_T (4)	D (Mpc) (5)	Scale (pc arcsec^{-1}) (6)
NGC 1300.....	SB(rs)bc	1.79 ± 0.01	11.11 ± 0.1	20.91	101.37
NGC 5992.....	S	0.94 ± 0.07	14.28 ± 0.15	126.4	612.8
NGC 6056.....	SB(s)0	0.96 ± 0.05	15.81 ± 0.08	157.1	761.6
NGC 6661.....	SA(s)0/a	1.24 ± 0.03	13.05 ± 0.16	58.3	282.63
NGC 6946.....	SAB(rs)cd	2.06 ± 0.01	9.61 ± 0.1	3.69	17.88
NGC 7013.....	SA(r)0/a	1.60 ± 0.02	12.40 ± 0.13	13.3	64.48
NGC 7217.....	(R)SA(r)ab	1.59 ± 0.02	11.02 ± 0.13	15.4	74.66
NGC 7479.....	SB(s)c	2.02 ± 0.01	10.35 ± 0.1	33.92	164.44
NGC 7606.....	SA(s)b	1.73 ± 0.02	11.51 ± 0.14	31.09	150.72
NGC 7723.....	SB(r)b	1.54 ± 0.03	11.94 ± 0.13	25	121.19
NGC 7753.....	SABbc	1.52 ± 0.03	12.83 ± 0.15	71.31	345.72

TABLE 2

SUMMARY OF OBSERVATIONS

Filter	Date	Exposure Time (s)	Seeing (arcsec)	Filter	Date	Exposure Time (s)	Seeing (arcsec)
NGC 1300:				NGC 7217:			
U	1990 Aug 23	1800	1.6	*U*	1990 Aug 17	200	1.6
B.....	1990 Aug 23	1200	1.3	*B*.....	1990 Aug 17	600	1.4
V.....	1990 Aug 23	300	1.1	*V*.....	1990 Aug 17	300	1.1
R	1990 Aug 23	400	1.1	*R*	1990 Aug 17	75	1.3
I	1990 Aug 23	400	1.2	*I*	1990 Aug 17	30	1.2
NGC 5992:				NGC 7479:			
U	1990 Aug 22	1800	1.8	*U*	1990 Aug 16	1800	1.3
B.....	1990 Aug 22	600	1.8	*B*.....	1990 Aug 16	1200	1.3
V.....	1990 Aug 22	300	1.6	*V*.....	1990 Aug 17	500	1.3
R	1990 Aug 22	150	1.4	*R*	1990 Aug 17	150	1.3
I	1990 Aug 22	150	1.3	*I*	1990 Aug 17	150	1.3
NGC 6056:				NGC 7606:			
U	1990 Aug 21	1800	1.7	*U*	1990 Aug 22	1800	1.6
B.....	1990 Aug 21	1200	1.6	*B*.....	1990 Aug 22	600	1.3
V.....	1990 Aug 21	600	1.3	*V*.....	1990 Aug 22	200	1.2
R	1990 Aug 21	250	1.3	*R*	1990 Aug 22	75	1.1
I	1990 Aug 21	250	1.3	*I*	1990 Aug 22	75	1
NGC 6661:				NGC 7723:			
U	1990 Aug 23	1800	1.8	*U*	1990 Aug 22	1800	1.6
B.....	1990 Aug 23	800	1.6	*B*.....	1990 Aug 22	1200	1.3
V.....	1990 Aug 23	400	1.4	*V*.....	1990 Aug 22	600	1.1
R	1990 Aug 23	400	1.3	*R*	1990 Aug 22	400	1.3
I	1990 Aug 23	150	1.3	*I*	1990 Aug 22	400	1
NGC 6946:				NGC 7753:			
U	1990 Aug 17	1800	1.7	*B*.....	1990 Aug 19	1500	1.4
B.....	1990 Aug 17	600	1.4	*V*.....	1990 Aug 19	300	1
V.....	1990 Aug 17	150	1.3	*R*	1990 Aug 21	100	0.9
R	1990 Aug 17	75	1.3	*I*	1990 Aug 21	100	1
I	1990 Aug 17	75	1.3				
NGC 7013:							
U	1990 Aug 22	1800	1.7				
B.....	1990 Aug 22	1200	1.7				
V.....	1990 Aug 22	150	1.5				
R	1990 Aug 22	50	1.5				
I	1990 Aug 22	50	1.5				

TABLE 3

CALIBRATION CONSTANTS

Galaxy	U	B	V	R	I
NGC 1300.....	28.3 ± 0.1	30.1 ± 0.1	29.86 ± 0.07	29.87 ± 0.03	29.23 ± 0.02
NGC 5992.....	28.7 ± 0.1	28.9 ± 0.1	28.74 ± 0.05	28.41 ± 0.03	27.99 ± 0.02
NGC 6056.....	28.7 ± 0.1	30.4 ± 0.1	30.24 ± 0.07	29.75 ± 0.04	29.03 ± 0.03
NGC 6661.....	27.3 ± 0.1	28.6 ± 0.1	28.86 ± 0.05	28.37 ± 0.03	27.877 ± 0.021
NGC 6946.....	...	...	26.64 ± 0.05	26.78 ± 0.03	26.61 ± 0.02
NGC 7013.....	28.2 ± 0.1	29.7 ± 0.1	28.30 ± 0.05	27.85 ± 0.03	27.46 ± 0.02
NGC 7217.....	27.5 ± 0.1	28.8 ± 0.1	27.33 ± 0.06	27.05 ± 0.05	26.20 ± 0.04
NGC 7479.....	28.5 ± 0.1	29.9 ± 0.1	29.69 ± 0.05	29.72 ± 0.03	29.11 ± 0.02
NGC 7606.....	29.5 ± 0.1	30.1 ± 0.1	29.39 ± 0.05	28.78 ± 0.03	28.11 ± 0.01
NGC 7723.....	28.8 ± 0.2	30.3 ± 0.1	30.01 ± 0.06	30.026 ± 0.03	29.38 ± 0.02
NGC 7753.....	...	30.2 ± 0.1	29.24 ± 0.04	28.53 ± 0.03	27.91 ± 0.01

axies have been included in this sample. Zaritsky & Lo (1986) suggested that the presence of nonradial forces, produced by oval distortions in the mass distribution, could be an efficient mechanism to drive gas toward the internal regions of the galaxy. One aspect of our project is to investigate the possible correlation between low nuclear or circumnuclear activity and the presence of triaxial structures.

In Table 1, we show the general parameters for the galaxies. Columns (1) and (2) are the NGC number and the morphological type from the RC3 (de Vaucouleurs et al. 1991), respectively. Column (3) is the logarithm of the 25th-magnitude isophotal diameter in units of 0.1 (RC3). Column (4) is the total apparent magnitude in the B band (RC3). The distance to the galaxy (obtained from the radial velocities given by the RC3 and using $H_0 = 75$ km s^{-1} Mpc^{-1}) is given in column (5), and column (6) gives the scale in parsecs per arcsecond.

Images were obtained at the prime focus of the 2.5 m Isaac Newton Telescope at the Roque de los Muchachos Observatory (ORM) on the island of La Palma, Spain, during 1990 August. A 400 × 590 pixel GEC6 CCD detector was used with a read noise of 8 e^- pixel^{-1}, a gain of 1 e^- ADU^{-1}, and a saturation level of 60,000 counts (Jorden 1988). For the focal ratio (f/3.29), the angular size of each pixel is 0.″54, which yields a field of 3.′5 in the north-south direction and 5.′2 east-west.

We have observations in the Johnson U, B, V, R, and I bands for all the galaxies in the sample. Observations were taken under photometric conditions. The observations are summarized in Table 2.

2.1. *Data Reduction*

Images were reduced using standard IRAF tasks. First, the bias level of the CCD (obtained from the overscan of each image and by taking images of zero exposure time) was subtracted from all exposures. We took a run of five to 10 bias images on each night. These were combined into a single image for each night using the ZEROCOMBINE task. The images were flat-fielded using twilight images taken in all filters at the beginning or end of each night.

The sky background level was removed by taking the mean of four or five 20 × 20 pixel regions free of sources. In those regions was also computed the typical standard deviation of the sky background, σ. The value of 3 σ determines the observed limiting magnitude for each galaxy. The galaxy NGC 6946 fills almost all of the CCD frame; for this reason, sky images were taken near to the object in order to obtain the sky level for that galaxy.

Cosmic-ray events were automatically subtracted using the COSMICRAYS task. Field stars were removed using the IMEDIT task. This replaces the star by the sky background level, evaluated in an annulus of radius 5 pixels around the star, and adds Gaussian noise. There is a bright star in the northern part of NGC 7013. The subtraction of this star was difficult, especially in the I band. For this reason, all the profiles for this galaxy do not include the region containing the star.

2.2. *Absolute Calibration*

The absolute calibration was performed by using the standards FZ 24 and FZ 108 (Laing, Sinclair, & Wood 1992). These stars were observed several times during each observing night and at different air masses. The standard chosen for the calibration of each galaxy was the closest one, in time and air mass, to the object. The calibration constant includes corrections for galactic inclination, atmospheric extinction, and Galactic extinction. No attempt was made to correct for internal extinction.

The first-order atmospheric extinction in the V band was taken from the measurements of the Carlsberg Automatic Meridian Circle at the ORM. We obtained the extinction in other filters by comparing this value with the aerosol measurement for the ORM (King 1985).

The first-order color term in the transformation equations derived by other authors (de Jong & van der Kruit 1994) gives maximum values of some hundredths of a magnitude for V, R, and I and of a tenth of a magnitude for the B band. These values were taken as part of the error in our calibration constants. The absolute calibration for the U, B, and V bands was based on the Landolt (1973) system, and for R and I on the Cousins (1976) system. The extinction of our Galaxy was taken from the RC3 in the B band (A_B). Using the Burstein (1979) law, the extinction in the other filters was

$$A_V = 0.76A_B\,, \tag{1}$$

$$A_R = 1.8A_V - 0.8A_B\,, \tag{2}$$

$$A_I = 2.62A_V - 1.62A_B\,. \tag{3}$$

For the U band, we used the Rieke & Lebofsky (1985) expression

$$A_U = 0.4A_B + A_V\,. \tag{4}$$

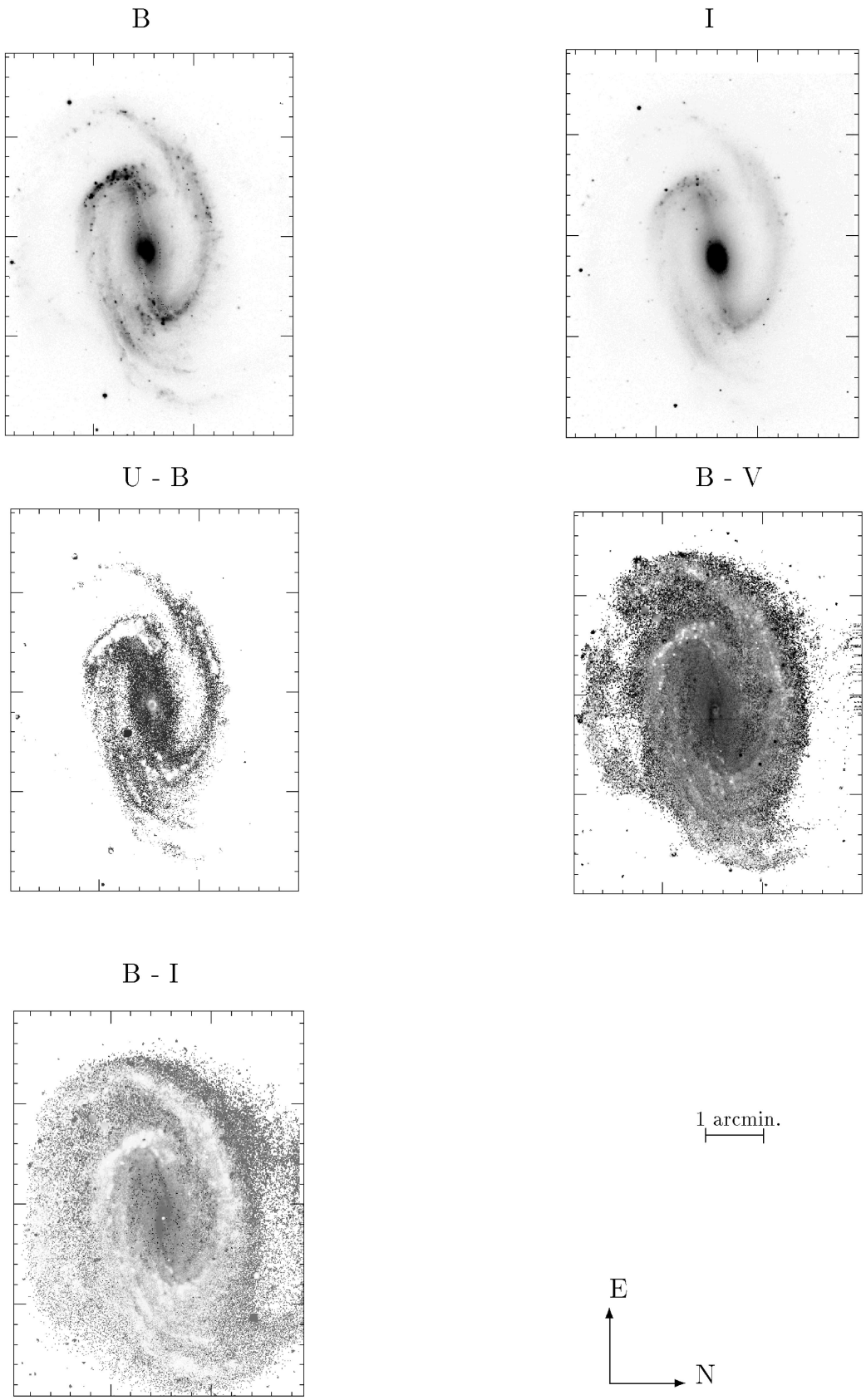

FIG. 1*a*

FIG. 1.—*B*- and *I*-band images and $U-B$, $B-V$, and $B-I$ color index maps for the galaxies of the sample. [*Figs. 1b–1k are presented in the electronic edition of the Astronomical Journal.*]

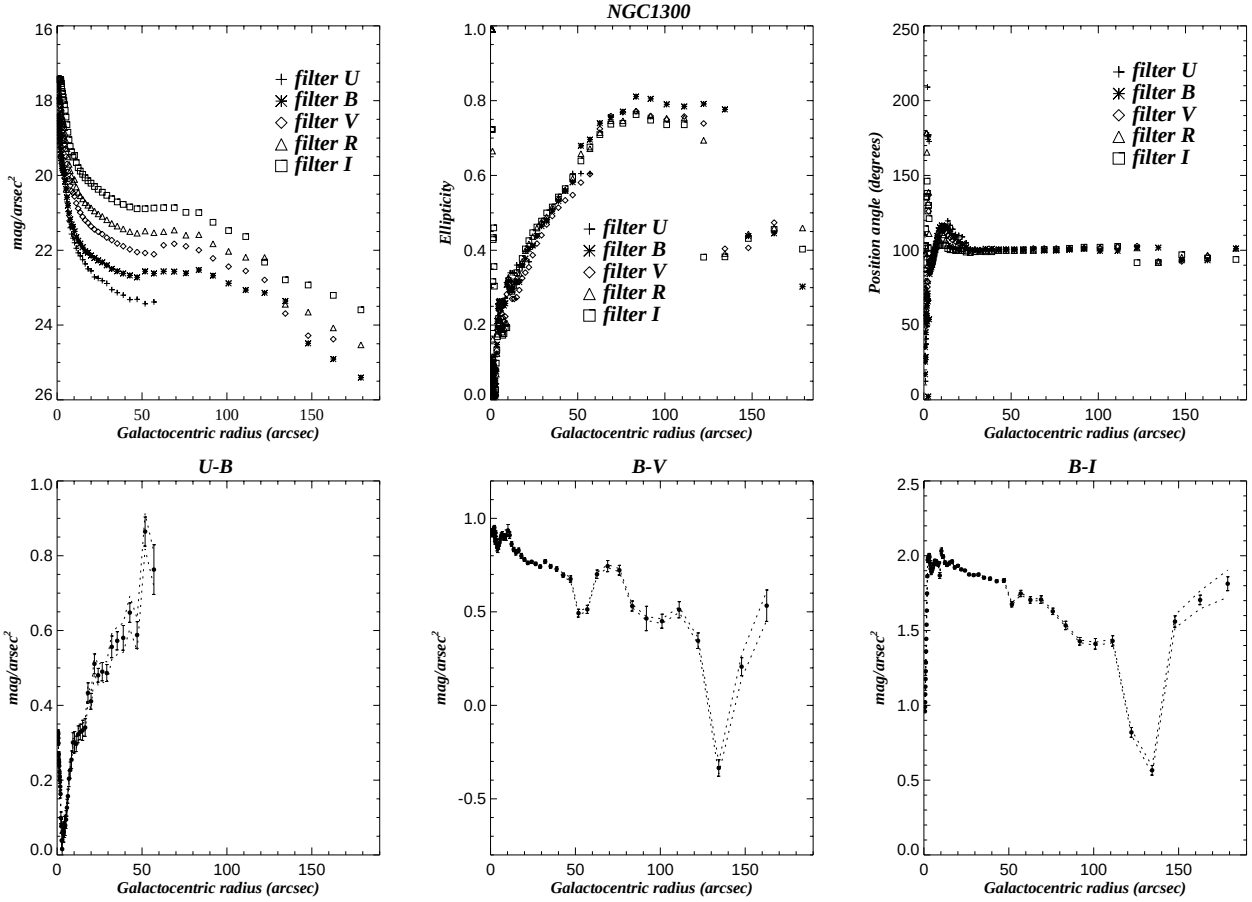

FIG. 2a

FIG. 2.—Surface brightness and $U-B$, $B-V$, and $B-I$ color index profiles. [*Figs. 2b–2k are presented in the electronic edition of the Astronomical Journal.*]

There are more recent studies about the Galactic extinction law (Cardelli, Clayton, & Mathis 1989). The differences $A(\lambda)/A(V)$ from the extinction law considered in this paper are about 0.01 in all filters. In Table 3 are given the calibration constants and associated errors for the galaxies in each filter.

3. RESULTS AND DISCUSSION

In Figure 1, we present the images of the galaxies in the B and I bands and the $U-B$, $B-V$, and $B-I$ color index maps. Images were previously aligned, and those with the best seeing were smoothed with a two-dimensional Gaussian filter according to the seeing of the other image. Where the images are red (*darker shades*), we can infer that the population is older or more metallic than in the bluer areas (*lighter shades*), or that we are observing starlight partly obscured by dust. This information is essential for determining accurate mass distributions in the galaxies.

Because of the inclination of the galaxies, their isophotes appear as ellipses. These ellipses were fitted using the ELLIPSE program from the IRAF package. This program uses an iterative algorithm described by Jedrzejewski (1987), which is similar to the method described by Kent (1983).

The azimuthally averaged surface brightness profiles in each band versus galactocentric radius, and the $U-B$, $B-V$, and $B-I$ color index profiles, are shown in Figure 2. The ellipticities (defined as $1-b/a$, b being the semiminor axis length and a the semimajor axis length for each ellipse) and the position angles (defined as the angle between the north direction and the major axis of each ellipse, measured in an eastward sense) of the ellipses as a function of galactocentric radius, together with their errors, are presented in Figure 3. The error of the intensity is the sum of the least-squares errors from the ellipse fitting plus the sky error due to its fluctuations, given (in magnitudes) by $\Delta m = 1.09(\sigma/I\sqrt{N})$, where I is the intensity of the corresponding isophote, σ is the typical deviation of the sky background, and N is the number of points of the ellipse. The maximum of these errors is 0.01 mag arcsec^{-2} for all the filters and all the galaxies of the sample. Another type of error is the systematic error determined by the subtraction of the sky background. The calculation and analysis of these errors were made following Silva & Elston (1994). The systematic errors are plotted in Figure 2 as dotted lines, and the random errors, Δm, are plotted as error bars.

The isophotal profiles provide information on the different structures that form the galaxy. For example, for a spiral galaxy that only shows a bulge and disk, the ellip-

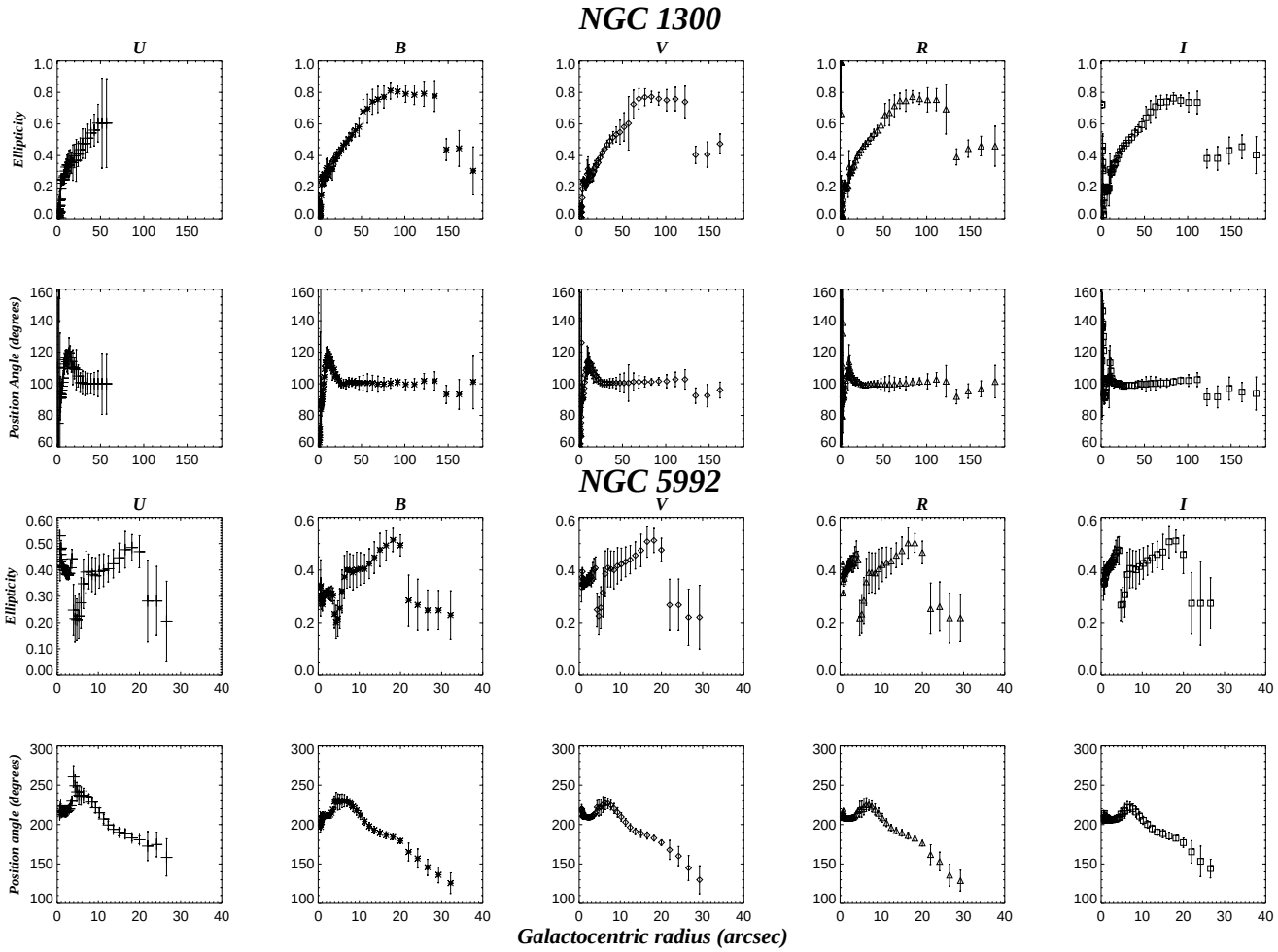

FIG. 3*a*

FIG. 3.—Ellipticity and position angle profiles for each bandpass. Error bars are overplotted. [*Figs. 3b–3f are presented in the electronic edition of the Astronomical Journal.*]

ticity of the isophotes is almost zero at the center and increases monotonically until reaching a constant value, which corresponds to the inclination of the disk (Varela et al. 1996). For a galaxy with a bar feature, the ellipticity grows from values of almost zero at the center to a local maximum at the end of the bar. It then falls to the ellipticity of the disk (Wozniak et al. 1995). In galaxies with two bars, the ellipticity first grows to a first local maximum corresponding to the secondary bar and then falls to a minimum before climbing again to a primary maximum, after which it decreases toward the ellipticity of the disk (Jungwiert, Combes, & Axon 1997).

We compared our photometric results (inclinations and position angles) with the values given by the RC3 and CCD values (if they existed in the literature) for the sample of galaxies. The position angle and inclination were computed by taking a mean of the last isophotes in the *B* band. In Figure 4, we show the comparisons among all these quantities. For the position angle and inclination, it is evident that our values and their errors are in very good agreement with the RC3 values. The weighted mean difference between our values and those of the RC3 for the inclination and position angle are $2\overset{\circ}{.}93 \pm 4\overset{\circ}{.}7$ and $4\overset{\circ}{.}00 \pm 11\overset{\circ}{.}3$, respectively.

Summarizing, we have obtained accurate surface photometry in the optical Johnson bandpass of a sample of 11 spiral galaxies. We have presented the observations and the calibration process for the images. The surface brightness, ellipticity, and position angle profiles obtained from the isophotal fitting are also shown, together with the color index profiles and color map images for the galaxies in the sample. The information provided in this paper will be used as a starting point for a program to derive the physical parameters and mass distributions of the galaxies, which will be the subject of a forthcoming paper.

This study was partly financed by Spain's DGES (grants PB97/0219 and PB97/0158).

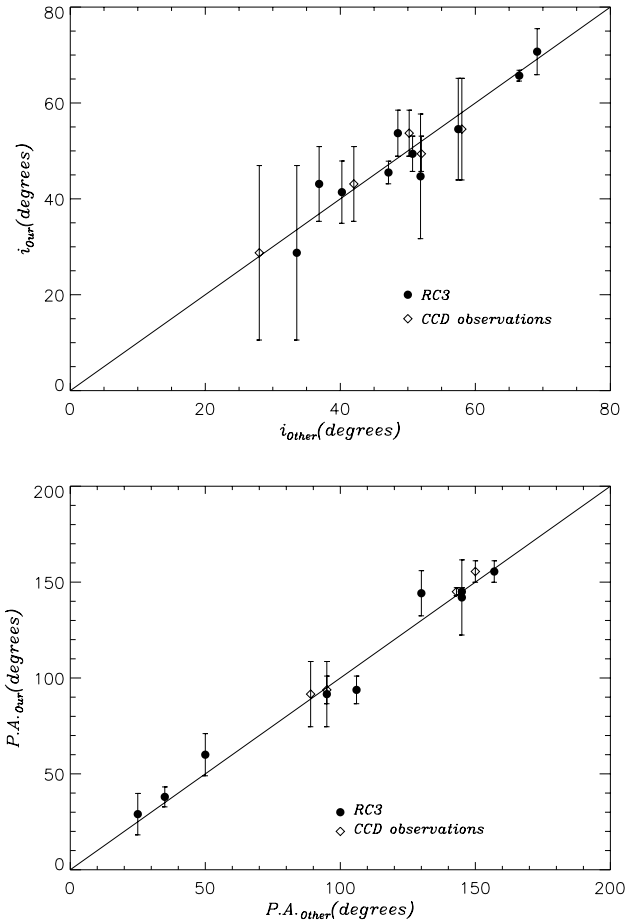

FIG. 4.—Comparison between our inclination (*top*) and position angle (*bottom*) values and those given by the RC3

REFERENCES

Andredakis, Y. C., & Sanders, R. H. 1994, MNRAS, 267, 283
Boroson, T. 1981, ApJS, 46, 177
Burstein, D. 1979, ApJ, 234, 435
Caon, N., Capaccioli, M., & D'Onofrio, M. 1993, MNRAS, 265, 1013
Cardelli, J. A., Clayton, G. C., & Mathis, J. S. 1989, ApJ, 345, 245
Cousins, A. W. J. 1976, MmRAS, 81, 25
de Jong, R. S. 1996a, A&AS, 118, 557
———. 1996b, A&A, 313, 45
de Jong, R. S., & van der Kruit, P. C. 1994, A&AS, 106, 451
de Vaucouleurs, G., de Vaucouleurs, A., Corwin, H. G., Jr., Buta, R. J., Paturel, G., & Fouqué, P. 1991, Third Reference Catalogue of Bright Galaxies (New York: Springer) (RC3)
Elmegreen, D. M., Elmegreen, B. G., Chromey, F. R., & Hasselbacher, D. A. 1996, ApJ, 469, 131
Evans, R. 1994, MNRAS, 266, 511
Freeman, K. C. 1970, ApJ, 160, 811
Hunter, J. H., Jr., Ball, R., Huntley, J. M., England, M. N., & Gottesman, S. T. 1988, ApJ, 324, 721
Jedrzejewski, R. I. 1987, MNRAS, 226, 747
Jorden, P. R. 1988, Basic Parameters of CCDs in Use at La Palma (ING La Palma Tech. Note 55) (version 3; La Palma: Inst. Astrofis. Canarias)
Jungwiert, B., Combes, F., & Axon, D. J. 1997, A&AS, 125, 479
Kent, S. M. 1983, ApJ, 266, 562
———. 1986, AJ, 91, 1301
———. 1987, AJ, 93, 816
King, D. L. 1985, Atmospheric Extinction at the Roque de Los Muchachos Observatory, La Palma (ING La Palma Tech. Note 31) (La Palma: Inst. Astrofis. Canarias)
Kormendy, J. 1977, ApJ, 214, 359
Laing, R., Sinclair, J., & Wood, R. 1992, Standard Star Lists Available at the ING (ING La Palma Tech. Note 85) (La Palma: Inst. Astrofis. Canarias)
Landolt, A. U. 1973, AJ, 78, 959
Peletier, R. F., Valentijn, E. A., Moorwood, A. F. M., & Freudling, W. 1994, A&AS, 108, 621
Peletier, R. F., Valentijn, E. A., Moorwood, A. F. M., Freudling, W., Knapen, J. H., & Beckman, J. E. 1995, A&A, 300, L1
Prieto, M., Aguerri, J. A. L., Varela, A. M., & Muñoz-Tuñón, C. 2000, A&A, submitted (Paper II)
Prieto, M., Beckman, J. E., Cepa, J., & Varela, A. M. 1992, A&A, 257, 85
Prieto, M., Gottesman, S. T., Aguerri, J. A. L., & Varela, A. M. 1997, AJ, 114, 1413
Rieke, G. H., & Lebofsky, M. J. 1985, ApJ, 288, 618
Rubin, V. C., Burstein, D., Ford, W. K., Jr., & Thonnard, N. 1985, ApJ, 289, 81
Rubin, V. C., Ford, W. K., Jr., & Thonnard, N. 1980, ApJ, 238, 471
Rubin, V. C., Ford, W. K., Jr., Thonnard, N., & Burstein, D. 1982, ApJ, 261, 439
Searle, L., Sargent, W. L. W., & Bagnuolo, W. G. 1973, ApJ, 179, 427
Silva, D. R., & Elston, R. 1994, ApJ, 428, 511
Simien, F., & de Vaucouleurs, G. 1986, ApJ, 302, 564
Simonneau, E., Varela, A. M., & Muñoz-Tuñón, C. 1993, J. Quant. Spectrosc. Radiat. Transfer, 49, 149
Stark, A. A. 1977, ApJ, 213, 368
Varela, A. M. 1992, Ph.D. thesis, Univ. La Laguna
Varela, A. M., Muñoz-Tuñón, C., & Simonneau, E. 1996, A&A, 306, 381
Wozniak, H., Friedli, D., Martinet, L., Martin, P., & Bratschi, P. 1995, A&AS, 111, 115
Zaritsky, D., & Lo, K. Y. 1986, ApJ, 303, 66